Live Imaging of Neuronal Degradation by Microglia Reveals a Role for v0-ATPase a1 in Phagosomal Fusion In Vivo

Peri, Francesca ; Nüsslein-Volhard, Christiane

Abstract: A significant proportion of neurons in the brain undergo programmed cell death. In order to prevent the diffusion of damaging degradation products, dying neurons are quickly digested by microglia. Despite the importance of microglia in several neuronal pathologies, the mechanism underlying their degradation of neurons remains elusive. Here, we exploit a microglial population in the zebrafish to study this process in intact living brains. In vivo imaging reveals that digestion of neurons occurs in compartments arising from the progressive fusion of vesicles. We demonstrate that this fusion is mediated by the v0-ATPase a1 subunit. By applying live pH indicators, we show that the a1 subunit mediates fusion between phagosomes and lysosomes during phagocytosis, a function that is independent of its proton pump activity. As a real-time description of microglial phagocytosis in vivo, this work advances our understanding of microglial-mediated neuronal degeneration, a hallmark of many neuronal diseases.

DOI: https://doi.org/10.1016/j.cell.2008.04.037

Cell

Live Imaging of Neuronal Degradation by Microglia Reveals a Role for v0-ATPase a1 in Phagosomal Fusion In Vivo

Francesca Peri[1,2,*] and Christiane Nüsslein-Volhard[1]
[1]Max Planck Institute for Developmental Biology, Spemannstr. 35, 72076 Tübingen, Germany
[2]Present address: EMBL Heidelberg, Meyerhofstraße 1, 69117 Heidelberg, Germany
*Correspondence: peri@embl.de
DOI 10.1016/j.cell.2008.04.037

SUMMARY

A significant proportion of neurons in the brain undergo programmed cell death. In order to prevent the diffusion of damaging degradation products, dying neurons are quickly digested by microglia. Despite the importance of microglia in several neuronal pathologies, the mechanism underlying their degradation of neurons remains elusive. Here, we exploit a microglial population in the zebrafish to study this process in intact living brains. In vivo imaging reveals that digestion of neurons occurs in compartments arising from the progressive fusion of vesicles. We demonstrate that this fusion is mediated by the v0-ATPase a1 subunit. By applying live pH indicators, we show that the a1 subunit mediates fusion between phagosomes and lysosomes during phagocytosis, a function that is independent of its proton pump activity. As a real-time description of microglial phagocytosis in vivo, this work advances our understanding of microglial-mediated neuronal degeneration, a hallmark of many neuronal diseases.

INTRODUCTION

Apoptosis plays a central role in sculpting tissues and regulating cell numbers. This is very well documented in the Central Nervous System (CNS) where a significant proportion of neurons undergo programmed cell death (Kuan et al., 2000; Nijhawan et al., 2000). To prevent the diffusion of damaging degradation products into the surrounding tissue it is essential that the dying neurons are quickly recognized and phagocytosed (Lauber et al., 2004; Platt et al., 1998). In the brain, this task is performed by a resident population of phagocytes, known as the microglia (Barron, 1995; Kettenmann, 2007). Microglia are the resident immune cells of the CNS. As such, they can protect the brain from infection by engulfing microorganisms, however, it is their ability to recognize, engulf and digest apoptotic neurons under physiological conditions that makes them important players in the formation and integrity of the nervous system. It is unclear how microglia detect apoptotic neurons in the healthy brain, but recent work has identified the P2Y12 purinergic receptor as the trigger of microglial chemotaxis and phagocytosis in response to neuronal injury in the brain (Koizumi et al., 2007; Tsuda et al., 2003). While many different stimuli may activate microglia, it is likely that the internal cellular machinery that is in place to efficiently digest neurons is the same whether these cells are engulfed during normal physiology or in response to pathological conditions.

Phagocytosis has long been studied at the cell biological level thanks to many elegant in vitro assays (Desjardins and Griffiths, 2003). These studies have establish that phagocytosis can be divided into several distinct steps: binding of the pray, formation of the phagosome and maturation of the latter to digest the ingested material. Importantly, the phagosome progressively fuses with other vesicles types, such as lysososmes, to acquire enzymes that are necessary for digestion. One important feature of phagosomal maturation is its acidification via the activity of proton pumps. This is a crucial step in the digestion process as the activity of digestive enzymes increases in a low-pH environment (Mellman et al., 1986). v-ATPases, the major cellular proton pumps, are multisubunit protein complexes consisting of the V0 and V1 sectors (Kawasaki-Nishi et al., 2003; Nishi and Forgac, 2002). Via ATP hydrolysis, the complex translocates protons into the vesicular lumen. While this is a well-established function for v-ATPases, it is now clear that the a1 subunit part of the v0 sector mediates membrane fusion events downstream of the t-SNARE docking of vesicles in a calcium/calmodulin-dependent manner (Bayer et al., 2003; Muller et al., 2002). In recent years, these data have been supported by in vivo evidence as it has been shown that in *D. melanogaster* and C. *elegans* neurons lacking the a1 subunit accumulate vesicles in their synaptic terminals suggesting that the V0 subunit may be involved in mediating vesicle fusion during exocytosis (Hiesinger et al., 2005; Liegeois et al., 2006).

Neuronal disposal by microglia is essential for normal brain development and physiology however, when uncontrolled, it characterizes several neurodegenerative disorders (Block et al., 2007). It is important to comprehend how under normal circumstances microglia interact with dying neuron in order to understand, prevent and cure the aberrations. We have developed tools to capture the behavior of microglia and their phagocytic organelles in living zebrafish brains. Here, we investigate how microglia act to phagocytose and digest neurons during brain

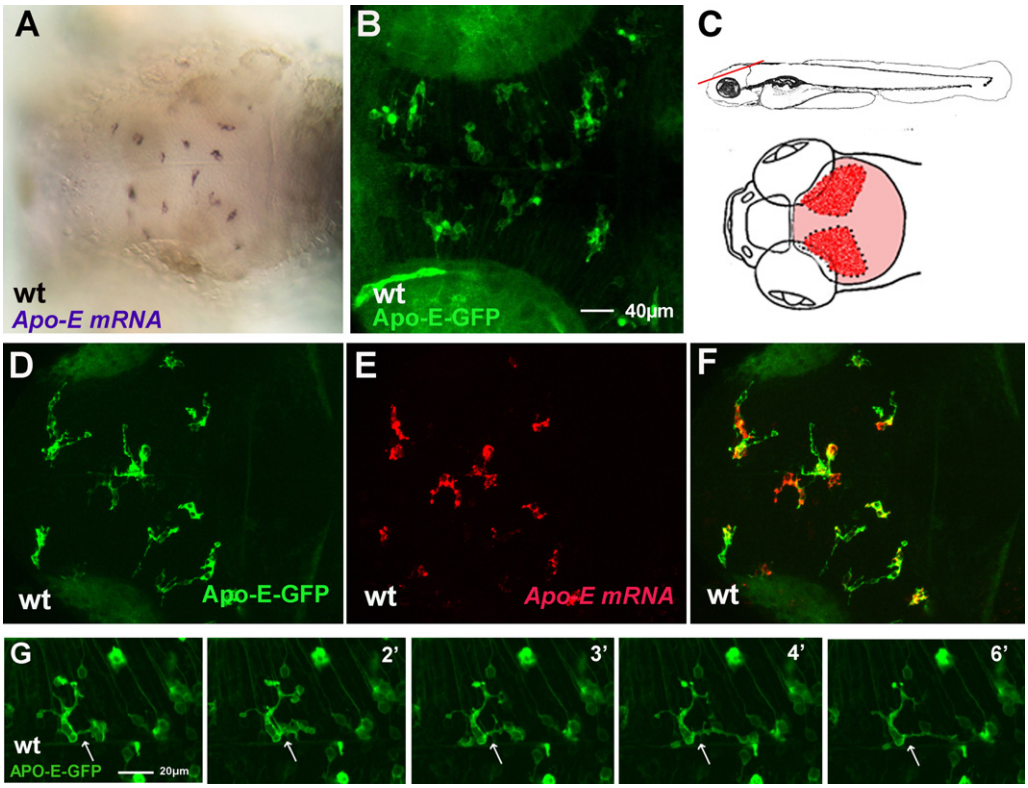

Figure 1. Microglia in the Zebrafish Brain

(A and B) Dorsal views of a 3 dpf (days post fertilization) embryonic wild-type brain. (A) Microglial expression of the *Apo-E* mRNA. (B) GFP expression under the control of the *Apo-E* locus.

(C) Schematic drawings of the regions of interest. Anterior is to the left. The upper panel represents a side view of a 3 dpf fish. The red bar marks the region and the depth at which confocal imaging has been performed. The lower part represents a dorsal view of the examined area (light red). The optic lobes are marked in dark red.

(D–F) Dorsal view of a 3 dpf wild-type embryonic brain. Double antibody (green [D]) and in situ (red [E]) staining show a perfect overlap between GFP and *apo-E* expression (F).

(G) Confocal time-lapse of one branching Apo-E wild-type microglial cell. Time is indicated in minutes.

development in vivo. Time-lapse confocal microscopy shows that this process is characterised by the fusion of vesicles. Blocking vesicular fusion leads to the accumulation of the apoptotic material inside the cell, with the cell being transformed into a bag of vesicles, unable to process collected material. As a first step toward understanding how microglia digest dying neurons, we have addressed the role of the v0-ATPase a1 subunit in this process in vivo. This has revealed a role in mediating vesicle fusion events during the process of phagocytosis. By applying pH indicators to living zebrafish embryos, we show that this requirement for the a1 subunit is independent of the acidifying role of the v0-ATPase complex.

RESULTS

In Vivo Imaging of Microglial Cells in the Zebrafish Embryo: Phagocytosis and Digestion of Neurons

In order to facilitate imaging of microglia we generated transgenic lines in which the GFP marker is expressed under the control of the *apolipoprotein-E* locus (Apo-E-GFP, Figure 1B), a previously described marker for zebrafish microglia (Figure 1A; Herbomel et al., 1999, 2001). To this aim, we introduced a membrane-bound GFP into the *apolipoprotein-E* locus. Transgenic lines recapitulate the *Apo-E* expression pattern and allow the in vivo morphology of these cells to be observed for the first time in the zebrafish (Figures 1B and 1D–1G). The APO-E-GFP cells are around 40 μm in size and display several features that are characteristic of mouse microglia (Nimmerjahn et al., 2005; Figures 1B and 1G). Mammalian microglia are highly branched cells characterised by filopodia and bulbous-tipped protrusions that undergo rapid cycles of formation, extension and withdrawal on a time scale of minutes. Likewise, the APO-E-GFP positive cells in the zebrafish brain show a similar branched morphology, with processes that extend and retract at a speed of 2.5 μm/min (Figure 1G and Movies S1 and S2 available online).

Previous work has shown that zebrafish microglia derives from a subset of macrophages, expressing the myeloid markers spi/pU1 and L-plastin (Herbomel et al., 1999). This macrophage pool can be depleted using an antisense morpholino shown to block translation of the *spi/pU1* transcription factor required to promote the differentiation of macrophages from their myeloid precursors (Rhodes et al., 2005). We directly tested whether these

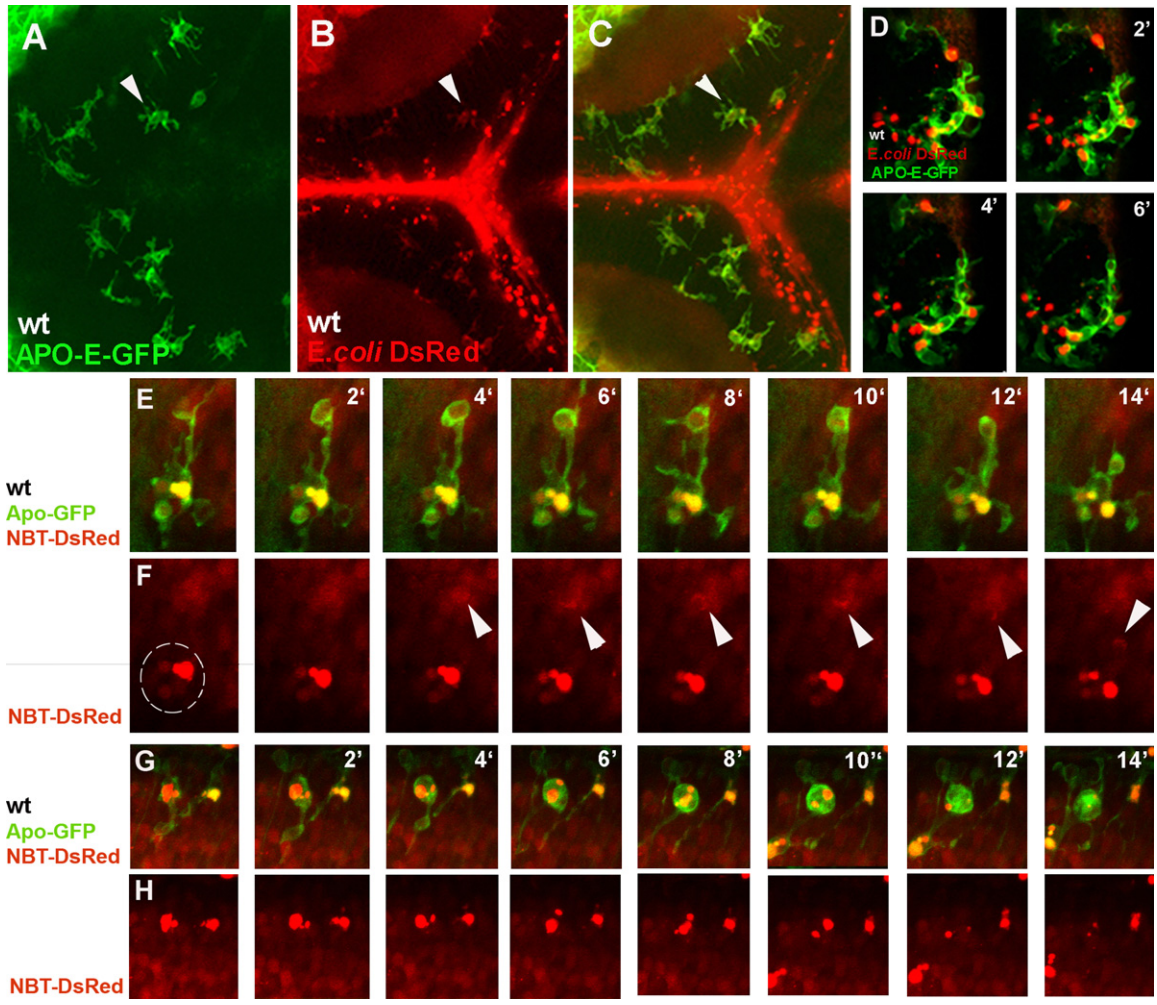

Figure 2. Microglia Phagocytose E. coli Bacteria and Neurons in the Brain

(A–C) Dorsal views of a 3 dpf (days post fertilization) embryonic wild-type brain. (A) Microglial labeled by Apo-E-GFP. (B) Red-labeled Gram-negative E.*coli* bacteria (DsRed Express, Clontech). (C) Merge. Red bacterial inclusions are present inside the microglia (white arrowhead).

(D) Confocal time-lapse of one Apo-E-GFP wild-type microglial cell collecting a red-labeled bacterial cluster (white arrowheads).

(E–H) Confocal time-lapse of one branching Apo-E-GFP wild-type microglial cell collecting (E) and (F) and digesting (G) and (H) NBT-DsRed neurons. Time is indicated in minutes. White arrowheads point to the neuronal material being collected by a phagosome, the dotted line encircles the neuronal material inside the microglia (F).

are the progenitors of the APO-E-GFP positive cells by depleting the macrophage population in the APO-E-GFP line. Injection of the *pU1* morpholino leads to the complete absence of Apo-E-GFP positive cells from the brain of the transgenic embryos, confirming the myeloid origin of these cells (Figures 4A and 4B).

We next asked whether APO-E-GFP positive cells are able to phagocytose pathogens, a characteristic function of microglial cells in the brain (Streit and Kincaid-Colton, 1995). We therefore injected red-labeled Gram-negative E.*coli* bacteria (DsRed Express, Clontech) into the ventricles of APO-E-GFP brains. Time-lapse imaging revealed that soon after injection, red bacterial inclusions are transported along cell extensions to the cell bodies of APO-E-GFP positive cells (Figures 2A–2C, white arrowhead and Figure 2D). Thus, the APO-E-GFP positive cells in the brain phagocytose invading microorganisms such as bacteria.

Another hallmark of microglia is that they can detect and phagocytose apoptotic neurons (Kuan et al., 2000). To observe such interactions between APO-E-GFP cells and surrounding neurons, we labeled all neurons in vivo by driving the DsRed Express marker under the control of a neuronal specific promoter (Figure 4I, NBT-DsRed). Crossing of the two transgenic lines reveals that bulbous-tipped protrusions on APO-E-GFP cells are phagocytic cups (around 5 μm in size, Movies S1 and S2), whose function is to phagocytose neurons transporting them to the cell body (Figures 2E and 2F and Movie S2). Collectively, these data strongly support our conclusion that the APO-E-GFP are the zebrafish equivalent of the mammalian microglia.

We turned our attention to the dynamics of neuronal phagocytosis by microglia. We observed that microglial cells repeatedly

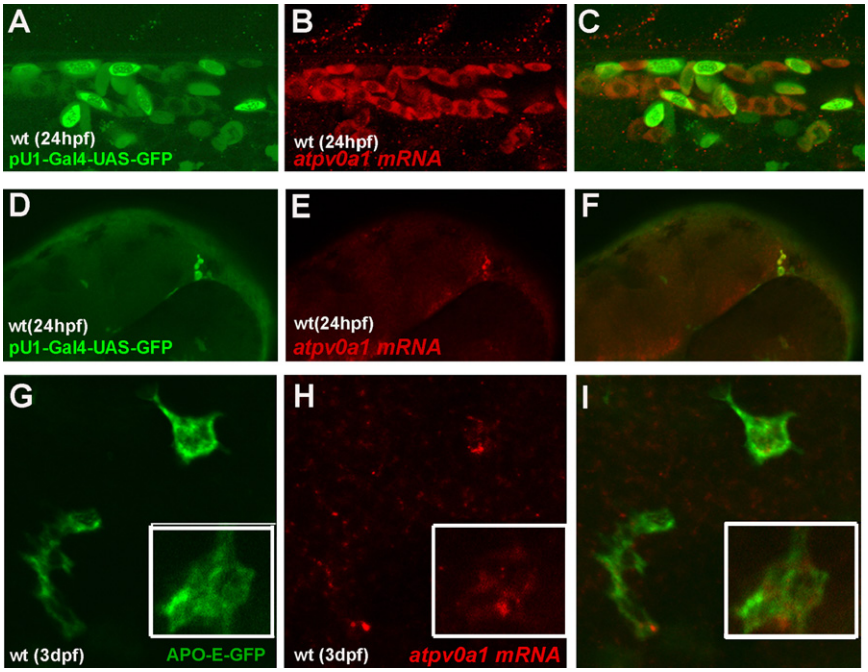

Figure 3. v0-ATPase a1 Expression in Macrophages and Microglia of the Zebrafish Embryo

(A–C) Side view of the wild-type fish trunk at 1 dpf (day post fertilization). (A) pU1-Gal4-UAS-GFP labels the myeloid lineage in green. (B) *atp6v0a1* expression in red (C) Merge.

(D–F) Side view of the wild-type fish head at 1 dpf (days post fertilization). (D) pU1-Gal4-UAS-GFP labels the myeloid lineage in green. (E) *atp6v0a1* expression is in red. (F) Merge.

(G–I) Dorsal view of the wild-type fish head at 3 dpf (days post fertilization). (G) Apo-E-GFP labels microglial cells in green. (H) *atp6v0a1* expression in red (I) Merge. In the bottom right corner is an enlargement of an APO-E-positive cell expressing *atp6v0a1* mRNA.

send out branches to collect NBT-DsRed labeled neurons, which accumulate as red clusters of different intensity (Figure 2F white arrowhead and dotted circle). These clusters are also strongly labeled with several markers for apoptosis such as AnnexinV-Cy5, CaspGLOW, acridine orange and TUNEL (Figures 4C and 4D and S3A–S3L, white arrowheads). Importantly, there is a tight correlation between the apoptotic clusters, whether marked with NBT-DsRed or the apoptosis indicators, and microglia, showing that APO-E-GFP labels all phagocytes that are active at this point in the fish brain (Figures 4H–4K). Finally, time-lapse imaging reveals that NBT-DsRed clusters are turned over showing that APO-E-GFP microglia engulf and digest neurons (Figures 2G and 2H and Movie S3).

The *atp6v0a1* Gene Is Expressed in Microglia and Their Precursors

One crucial event during phagocytosis is the progressive acidification of phagosomes. The vacuolar (V-type) ATPases, consisting of a V1 and V0 complexes, are the major proton pumps involved in the acidification of intracellular compartments. By analyzing the zebrafish genome we identified one zebrafish homolog of the a1 subunit (*atp6v0a1;* NP 997837). In order to pinpoint its in vivo expression we performed in situ hybridization against the *atp6v0a1* transcript in embryos in which myeloid cells and microglia are labeled by GFP expression. To label the myeloid precursors of microglia, we have generated a pU1-Gal4-UAS-GFP transgenic line in which GFP is expressed under the control of pU1, an early macrophage marker. Indeed, the pU1-Gal4-UAS-GFP positive cells that localize along the trunk and move toward the brain to become microglia express *atp6v0a1* (Figures 3A–3F). At 3 days post fertilization, once the microglial population is established, APO-E-GFP cells show *atp6v0a1* expression (Figures 3G–3I). This shows that the a1 subunit is present in both microglia and in myeloid cells.

Neuronal Apoptotic Foci Are Larger in atp6v0a1 Morpholino Knockdowns

We next addressed the function of the *atp6v0a1* during the turnover of neurons by microglia by knocking-down its translation via the injection of antisense morpholino oligonucleotides (atp6v0a1-MO, a1-MO; Nasevicius and Ekker, 2000). Morpholino efficacy was assayed by western blot analysis and this shows that the expected 116kDa band, presents in extracts of 3 dpf uninjected embryos, is absent in embryonic extracts obtained from atp6v0a1 3 dpf knockdown embryos, confirming the efficacy of the morpholino mediated knockdown (Figure 4G). Furthermore, to test the specificity of the a1-MO we have fused its target sequence to GFP and a 5 base mismatch control sequence to dtTomato. Coinjection of these fusion mRNAs into one-cell stage embryos gave strong green and red fluorescence after 6 hr (Figures S1A–S1D). Whenever the coinjection of both mRNAs was followed by the injection of the a1-MO, the embryos were red but not green, showing the specific binding of the a1-MO to its target sequence (Figures S1E and S1F). Moreover, the injection of the control morpholino does not block the translation of either of the two reporter constructs (Figures S1G and S1H).

In APO-E-GFP/NBT-DsRed embryos phagocytosed neurons appear as a strong red cluster with low power objectives (Figure 4I, white arrowhead). Closer inspection reveals that each cluster comprises 4-to-12 smaller vesicles of neuronal material (Figures 2F, 4I and 4J, and 4F). In morphant APO-E-GFP/NBT-DsRed embryos, the total number of clusters per embryo is comparable to the wild-type, however each cluster is considerably larger and is formed by 10 to 20 smaller spots (Figure 4, compare 4I and 4J with 4M and 4N, white arrowheads, quantified in Figure 4E and 4F).

Finally, we have used a second morpholino that blocks the splicing of the first intron from the v-ATPase transcript and we have confirmed the specificity and efficacy of the knockdown by monitoring a size-shift in the transcript produced from the vAtpase gene. This shows an identical phenotype to the ATG morpholino, albeit with lower penetrance (Figure S2).

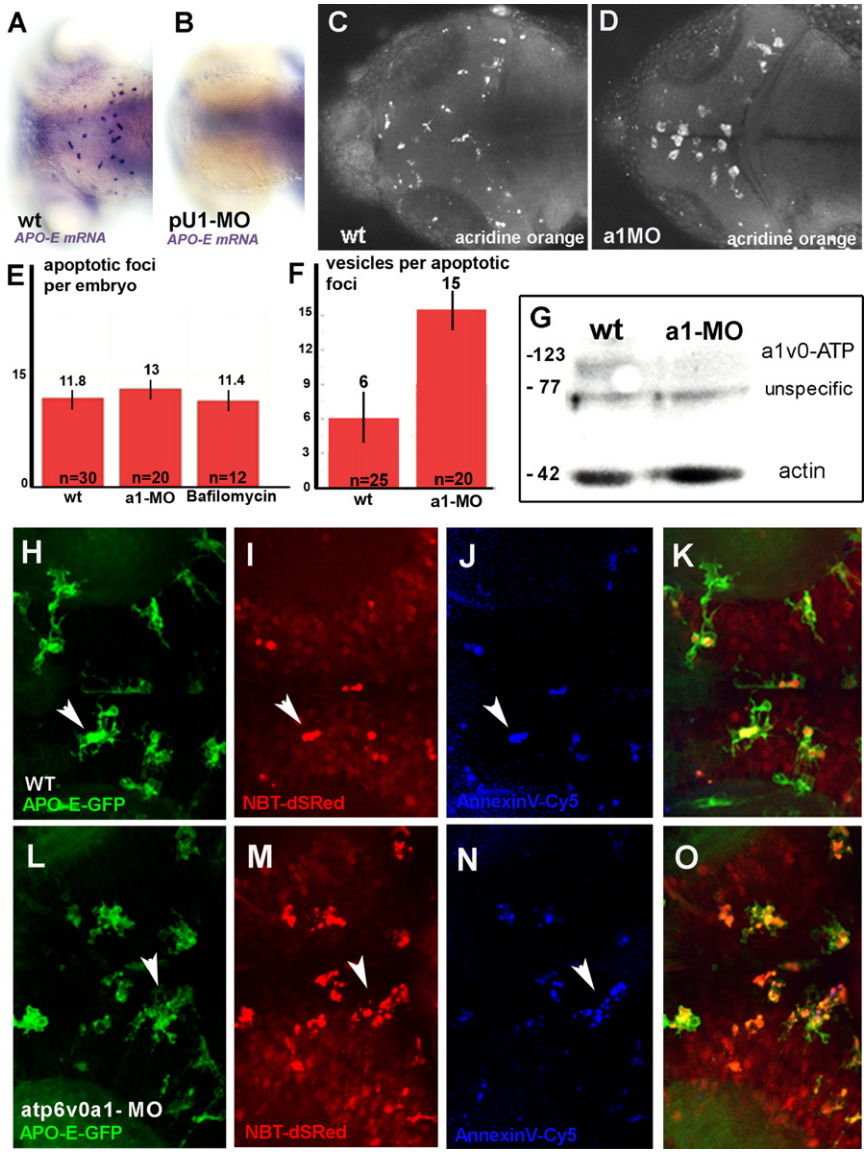

Figure 4. Accumulation of Apoptotic Neuronal Material in v0-ATPase a1 Knocked-Down Microglia

(A and B) Apo-E-expressing cells have a myeloid origin. Dorsal view of the wild-type fish head at 3 dpf (days post fertilization). (A) *apo-E* mRNA expression in the wild-type embryo. (B) *apo-E* mRNA is not detectable in embryos injected with a morpholino directed against the pU1 transcription factor, whose activity is required for myeloid cells specification.

(C and D) Dorsal view of the wild-type fish head at 3 dpf (days post fertilization). Acridine orange stainings detect apoptosis in the CNS. Levels of apoptosis within the CNS are comparable in wild-type (C) and atp6v0a1-MO embryos (D).

(E) Quantification of the number of apoptotic clusters per embryo. The values are comparable between wild-type, atp6v0a1-MO and Bafilomycin-A1 treated microglia. The data represent the average ± SD of ten independent experiments.

(F) Quantification of the apoptotic cluster size. Apoptotic foci in atp6v0a1-MO embryos are three times larger then in the wild-type. These values were obtained by counting the number of red vesicles per cluster in different experiments. The data represent the average ± SD of ten independent experiments.

(G) Western blotting analysis using a polyclonal antibody directed against v0-ATpase a1. This shows that the expected 116kDa band, presents in extracts of 3 dpf uninjected embryos, is absent in extracts obtained from atp6v0a1 3 dpf knockdown embryos. This confirms the efficacy of the morpholino mediated knockdown.

(H–K) Dorsal view of the wild-type fish head at 3 dpf (days post fertilization). Foci of apoptotic neurons are found inside wild-type microglia. (H) Apo-E-GFP expression. (I) NBT-dSRed expression. (J) AnnexinV-Cy5 labeling of apoptotic clusters. (K) Merge. White arrowhead points at one single apoptotic neuronal cluster.

(L–O) Dorsal view of the fish head at 3 dpf (days post fertilization) in *atpv0a1* morpholino injected embryos. Foci of apoptotic neurons are larger then in wild-type. (L) Apo-E-GFP expression. (M) NBTdSRed expression. (N) AnnexinV-Cy5 labeling of apoptotic clusters. (O) Merge. White arrowhead points at one single apoptotic neuronal cluster. The size of the cluster is larger when compared to the wild-type.

Atp6v0a1-MO Microglia Are Unable to Digest Apoptotic Neurons

An increase in the amount of apoptotic material inside morphant microglia can be caused by augmented neuronal apoptosis. However, by performing time-course experiments with several markers and vital dyes for apoptosis, such as Annexin-Cy5, Acridine orange, TUNEL and CaspGLOW, we did not detect a difference in the levels of apoptosis within the CNS between wild-type and atp6v0a1-MO embryos (Figure 4 compare 4C and 4J with 4D and 4N and Figures S3A–SF, SG–SK, and SL). In both wild-type and morphant embryos, the apoptotic staining is detectable almost exclusively inside microglia. Interestingly, in embryos where neuronal apoptosis increases significantly, dying neurons are found throughout the brain, a phenotype that is clearly distinct from the increased cluster size observed here (Liu et al., 2003; Campbell et al., 2006). Furthermore, an increase in neuronal apoptosis or neuronal degeneration causes a dramatic expansion in microglial number, a phenomenon that is called microgliosis (Nijhawan et al., 2000; F.P., unpublished data).

These data raise the possibility that the large amount of apoptotic material within atp6v0a1-MO microglia is caused by the inability of these cells to digest what they have engulfed. To test this hypothesis we have conducted an Annexin-Cy5 'pulse-chase' experiment to compare the dynamics of neuronal degradation within wild-type and morphant microglia. Time-lapse imaging allowed us to compare how efficiently wild-type

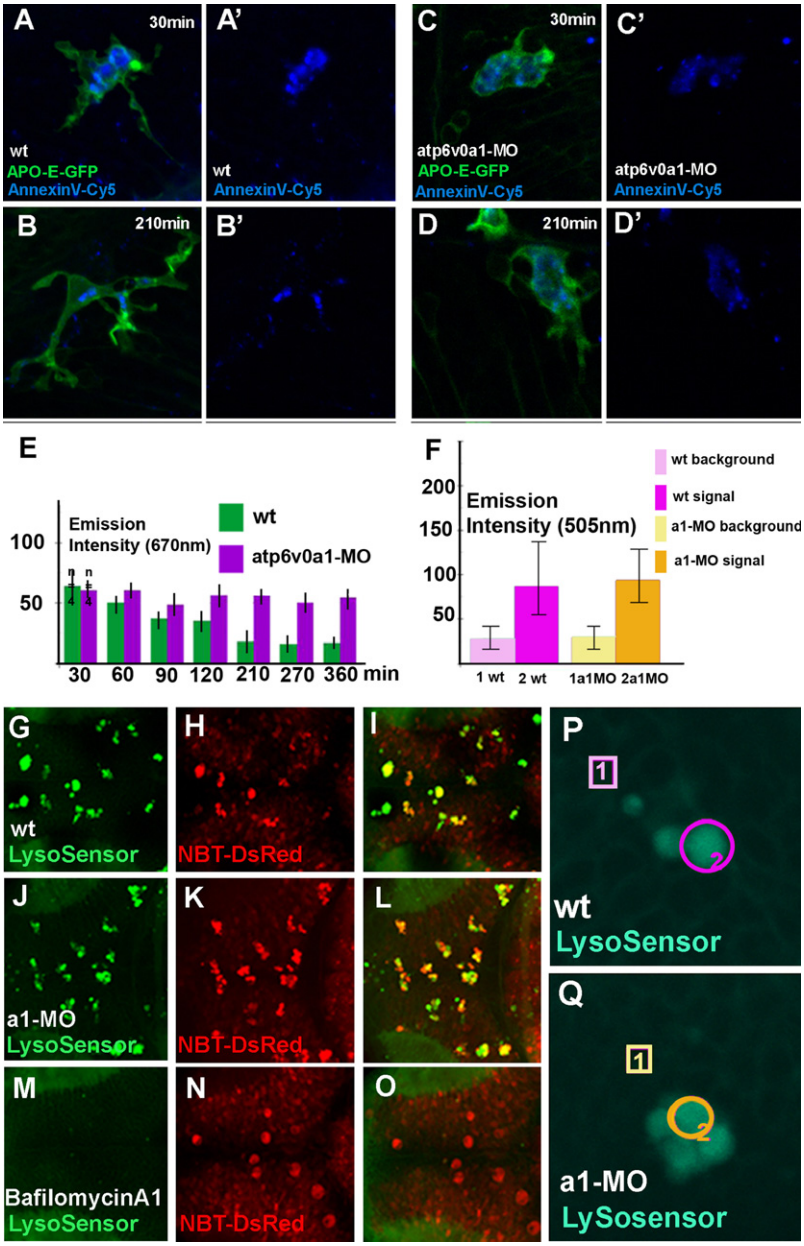

Figure 5. v0-ATPase a1 Knocked-Down Microglia Are Unable to Digest Apoptotic Neurons, However Vesicular Acidification Is Not Effected

(A and B) Two time points (0 and 210 min) of confocal time-lapse of one APO-E-GFP wild-type microglial cell containing apoptotic material labeled by AnnexinV-Cy5 binding. Time is in minutes. (A′ and B′) AnnexinV-Cy5 labeling in the same microglial cell.

(C and D) Two time points (0 and 210 min) of confocal time-lapse of one APO-E-GFP v0-ATPase a1 knocked-down microglial cell containing the apoptotic material labeled by AnnexinV-Cy5 binding. Time is in minutes. (C′ and D′) Confocal time-lapse of AnnexinV-Cy5 labeling in the same microglial cell.

(E) Quantification of fluorescent intensity emission values at 670 nm (AnnexinV-Cy5) in wild-type microglia (green bars) and *atp6v0a1* knocked-down microglia (purple bars). Error bars indicate standard deviation. Over time, AnnexinV-Cy5 staining disappears only from wild-type embryos. The data represent the average ± SD of four independent experiments.

(F) We have measured fluorescent intensity values at 505nm (LysoSensor) in several wild-type vesicular clusters.

(G–I) Dorsal views of a 3 dpf (days post fertilization) embryonic wild-type brain. (G) LysoSensor. (H) NBT-DsRed. (I) Merge. There is partial colocalization between acidic vesicles (green) and apoptotic cluster (red).

(J–L) Dorsal views of a 3 dpf (days post fertilization) embryonic v0-ATPase-a1 knocked-down brain. (J) LysoSensor. (K) NBT-DsRed. (L) Merge. Acidic vesicles can be detected in v0-ATPase a1 knocked-down and they colocalize with the neuronal apoptotic clusters.

(M–O) Dorsal views of a 3 dpf (days post fertilization) embryonic wild-type brain treated with Bafilomycin A1. (M) LysoSensor. (N) NBT-DsRed. (O) Merge. After Bafilomycin A1 treatment vesicles are no longer acidic and are not labeled by the LysoSensor.

(P) and (Q) Examples of wild-type (P) and atpv0a1-MO (Q) acidic vesicular clusters, (purple circle [P]) and in atpv0a1-MO (yellow circle [Q]). We have also measured background fluorescent emission at 505nm in wild-type (purple square [P]) and in atpv0a1-MO (yellow square [Q]). Values from several different experiments have been plotted. Error bars indicate standard deviation.

and morphant microglia turnover these bulk-labeled neurons by monitoring the shift in Annexin-V-Cy5 fluorescence intensity at 30 min intervals. While there is a progressive decrease in the amount of AnnexinV-Cy5 fluorescence, present in wild-type cells, in morphant microglia emission stale (Figure 5 compare 5A and 5B, 5A′ and 5B′, with 5C and 5D, 5C′ and 5D′, and 5E). Thus, microglia with reduced atp6v0a1 activity are phagocytic but display a specific block in the digestion of apoptotic neurons.

In Vivo Vesicular pH Measurement Shows that Vesicular Acidification Takes Place in the Absence of atp6v0a1 Activity

Given that v-ATPases are the major intracellular proton pumps, one possible explanation for the lack of neuronal digestion in atp6v0a1-MO microglia is a block in phagosomal acidification. The fluorophore LysoSensor GREEN-DND-189 (LysoSensor) is a reliable indicator of vesicular acidification, used in cell cultures to label acidic organelles and to monitor pH gradients (Harris and Cardelli, 2002). The LysoSensor dye labels microglia with remarkable specificity after a quick 5 min incubation. Surprisingly, LysoSensor also labels acidic compartments inside morphant microglia with an intensity emission that is indistinguishable from wild-type (Figures 5G–5I and 5J–5L, compare 5P with 5Q and 5F), This indicates that acidification of vesicles occurs also in the absence of a1 v0-ATPase activity in morphant microglia. Thus, failure in digesting apoptotic neurons in atp6v0a1-MO embryos is not caused by a block in vesicular acidification.

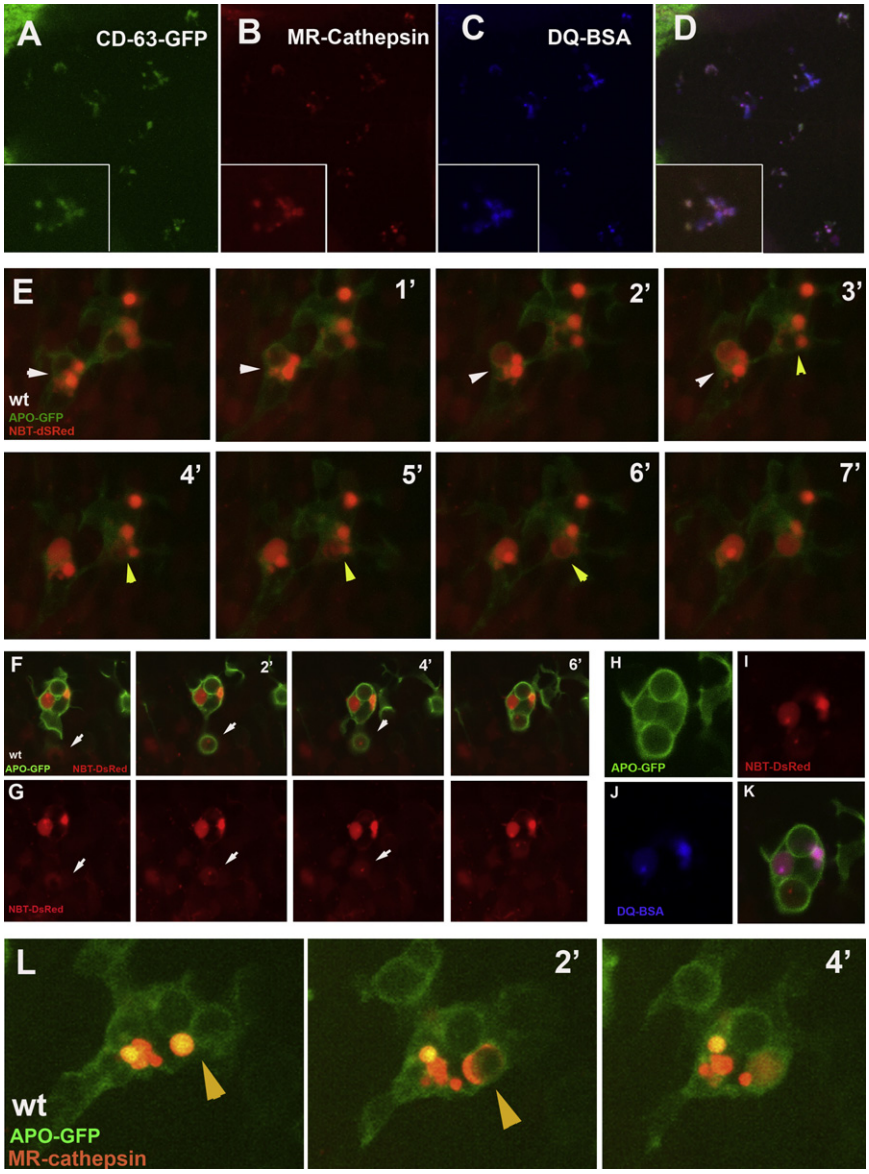

Figure 6. Time-Lapse Analysis of Vesicular Fusion Events

(A–D) Colocalization of the genetically encoded lysosomal marker CD63/Lamp-GFP3 (I) with the lysosomal membrane permeable dyes MR-Cathepsin (J) and DQ-BSA (K). In the bottom left corner an enlargement is presented.

(E) Confocal time-lapse of a single wild-type APO-GFP microglia and NBT DsRed neurons. Phagosomes of different intensity containing apoptotic neuronal material fuse (white arrowheads). Fusion is visible due to the spreading of dye from one vesicle into the other. Time is in minutes.

(F and G) Confocal time-lapse of a single wild-type APO-GFP microglia and NBT DsRed neurons. The cell branches out to collect neuronal material and a new phagosome forms (white arrowhead).

(H–K) The same cell as in (F). APO-GFP (H). NBT-DsRed (I). DQ-BSA (J). Merge (K). The newly formed vesicle is a phagosome and it is not yet labeled by the DQ-BSA dye.

(L) Confocal time-lapse of a single wild-type APO-GFP microglia whose lysosomes are labeled in red by MR-chatepsin. The yellow arrowhead points at a fusion event between a lysososme (red) and a phagosome (green). Time is in minutes.

In order to confirm that LysoSensor labeling is a reliable readout of v-ATPase acidification in this context, we took advantage of a widely used small molecule inhibitor of v-ATPase proton pump, Bafilomycin A1 (Bowman et al., 2004). As shown in Figure 5, adding Bafilomycin A1 to the fish medium completely abolishes LysoSensor labeling within microglia, indicating that this dye can indeed be used as a bone fide indicator of v-ATPase organelle acidification in living animals (Figure 5M–5O).

To understand how wild-type and morphant phagosomes become acidified, we have tracked their behavior by time-lapse imaging (Figures 7A and 7B and Movies S4 and S5). Two-color time-lapse imaging reveals that in both wild-type and morphant microglia, phagosomes turn acidic approximately 10 min after their formation. (Figures 7A and 7B and Movies S4 and S5; yellow arrowheads). Importantly, this event occurs autonomously and is independent from fusion with neighboring acidic vesicles. Early phagosomal acidification that is independent from fusion has been previously documented and is suggested to be mediated by vacuolar ATPases present on the plasma membrane of granulocytes and macrophages (Bouvier et al., 1994; Grinstein et al., 1992; McNeil et al., 1983; Geisow et al., 1981).

In wild-type cells after acidification phagosomes start fusing (Figure 7A and Movie S4). These events are also visible during time-lapse imaging of NBT-DsRed phagosomes. Here, when vesicles of different intensity merge we can observe a spreading of the dye from one compartment to the other resulting in an equilibration of intensity that renders fusion events more conspicuous (Figure 6E, Movie S7, white arrowheads). However, in morphant microglia, even although phagosomes are acidic, we never see them fuse (Figure 7B, Movie S5, white asterisks). To quantify fusion events we counted the number of GFP labeled vesicles over 4 hr time-course. In wild-type, the number of vesicles per cell fluctuates, due to vesicle formation and fusion. By contrast, in the morphant microglia vesicle number either remains constantly high or increases during the same period of time (Figure S4). Therefore knock-down of the a1 subunit does not block the acidification of organelles but rather prevents their fusion.

Atp6v0a1 Activity Is Required to Mediate Heterotypic Fusion Events during Phagocytosis

A key event during phagocytosis is the heterotypic fusion between phagosomes, that carry the material to digest, and

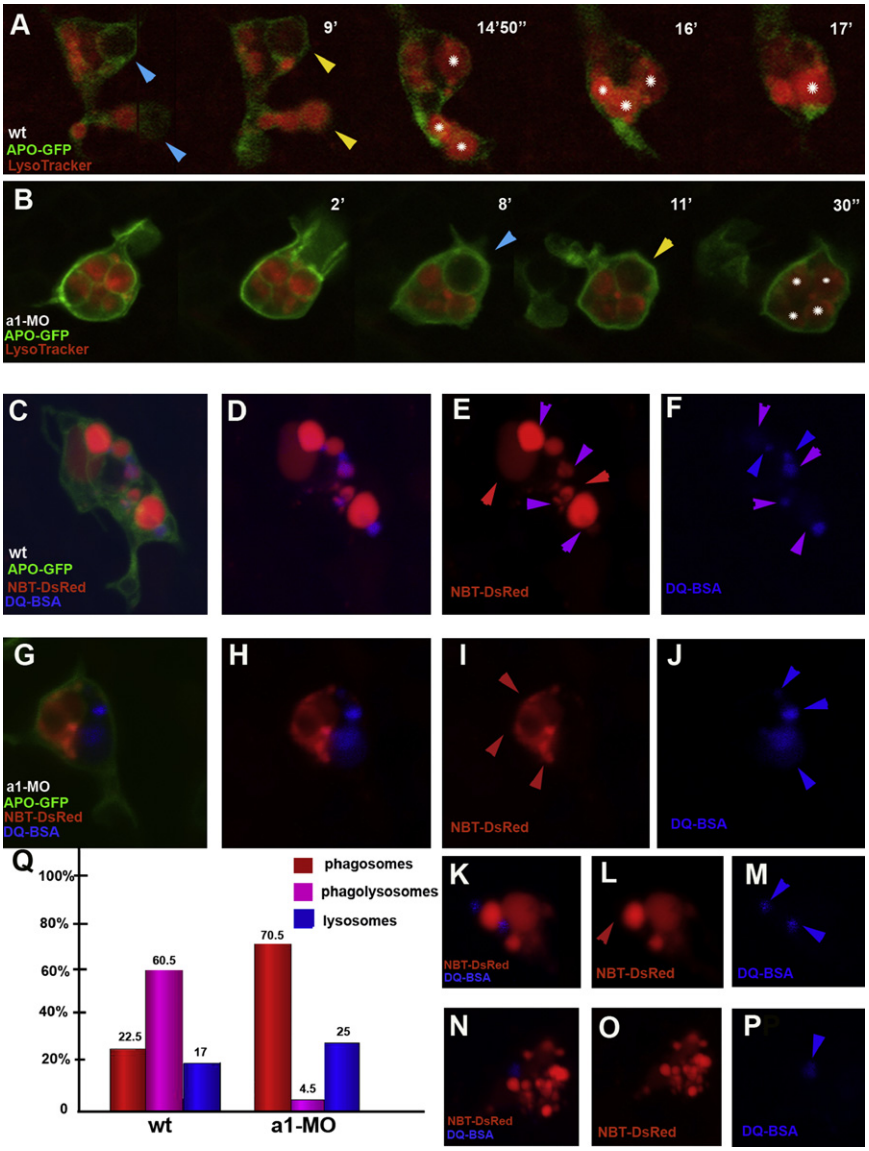

Figure 7. Phagolysosomal Fusion Defects in *atp6v0a1* Morpholino Knock-Down

(A) Confocal time-lapse analysis of wild-type (A) and atp6v0a1-MO microglia (B) microglia in 3 dpf brains. Time is indicated in minutes and seconds. Microglia are in green marked by GFP expression (Apo-E-GFP) while acidic endocytotic vesicles are marked in red by the LysoTracker. Blue arrowheads mark the formation of phagosomes. Yellow arrowheads mark phagosomal acidification (the vesicle turns red). White asterisks label single acidic vesicles. Fusion between acidic phagosomes is only observed in wild-type.

(C–P) Heterotypic vesicular fusion in wild-type (C–F) and in atp6v0a1-MO microglia (G–P). (E, I, L, and O) NBT-DsRed labeling of phagosomes and phagolysosomes. (F, J, M, and P) DQ-BSA labeling of lysosomes and phagolysosomes. (D, H, K, and N). Merge. Phagosomes are marked by red arrowhead, lysosomes by blue arrowheads and phagolysosomes by purple arrowheads. Phagolysosomes (purple) are only observed in the wild-type (C and D).

(Q) Percentage of the number of phagosomes (red bars), lysosomes (blue bars) and phagolysosomes (purple bars) present in wild-type (n = 15) and morphant cells (n = 15).

lysosomes, that provide the enzymes required for digestion. To determine if during phagocytosis the v0-Atpase a1 subunit mediates the fusion between these two different vesicle types, we have addressed the behavior of these organelles in living fish brains. To this aim, we have first labeled the lysosomes using MR-Cathepsin, whose red fluorescence is quenched until cleaved by enzymes found only in lysosomes (Figure 6L). We confirmed that MR-Cathepsin localizes specifically to lysosomes using a genetically encoded lysosomal marker, CD63/Lysosomal-Membrane-Associated-Protein-3-GFP (Figures 6A and 6B; de Saint-Vis et al., 2000; Blott et al., 2001). As shown in Figure 6, phagosomes forming at the plasma membrane of APO-GFP microglia (green) fuse with MR-Cathepsin lysosomes (red). This fusion event is marked by the spreading of the red dye from one vesicle type into the other (Figure 6L and movie 8). In order to quantify these events both in wild-type and morphant brain it was important to label at the same time microglial cell boundaries, phagosomes, lysosomes and phagolysosomes. We therefore turned to DQ-BSA, which emits fluorescence at the far-red end of the spectrum and allows simple spectral separation from the two transgenic markers. Once again, we confirmed the specificity of this dye for lysosomes by showing that it colocalizes with the CD63/LAMP3-GFP and with MR-Cathepsin in lysosomes (Figures 6A–6D). Using DQ-BSA, we can color-code and quantify three vesicle types within wild-type microglia, highlighting phagosomes in red (NBT-DsRed, red arrowheads), lysosomes in blue (DQ-BSA, blue arrowheads) and phagoolysosomes in purple, resulting from the fusion between red phagosomes and blue lysosomes. In wild-type embryos, phagolysosomes are the most prevalent compartment, providing 60% of the total vesicular population and out-numbering the other two by approximately 3:1 (Figures 7C–7F and 7Q and Movie S9). Strikingly, in a1-MO morphant microglia phagolysosomes are essentially absent, representing less than 5% of all quantified vesicles (Figures 7G–7P and Movie S10). In these embyos there is a dramatic increase in the number of unfused phagosomes, which here represent over 70% of the total vesicles (Figures 7N–7P, 7Q, and Movie S10).

We conclude that the activity of Atp6v0a1 is required for the formation of phagolysosomes, the digestive compartment, an event that is crucial for the turnover of apoptotic neurons by microglia during brain development.

DISCUSSION

Microglia in the Zebrafish

We have presented an in vivo description of zebrafish microglia using labeling with transgenic APO E -GFP. While microglia have not been studied in detail in this organism, several lines of evidence show that APO-E-GFP positive cells are zebrafish microglia. These include their myeloid origin, the fact that the GFP positive cells share morphological and behavioral features with mammalian microglia and, most importantly, their capacity to phagocytose bacteria and dying neurons. Several features make this model system well suited for studying the in vivo dynamics and functions of microglia. While the embryonic fish brain is small (400 μm wide), the microglia cells are remarkably large (40–50 μm wide) and their small number (around 30 cells) allows easy imaging of the entire cellular network they form in order to monitor the brain. We found that these cells are already in position and functional by three days of development, allowing us to study their response to the natural phenomena of neuronal cell death in a completely intact system.

In a recent publication Kurant et al. (2008) have shown that in *Drosophila melanogaster*, a specie which has not evolved a dedicated lineage for neuronal removal, apoptotic neurons are engulfed by neighboring glia. Also in vertebrates, glia have been shown to be able to phagocytose neurons, although at a much slower rate (Kurant et al., 2008; Parnaik et al., 2000). One striking and consistent finding from our analysis is the tight coupling between the apoptotic neurons and the microglia. Every time we observe dead neurons in the zebrafish brain—whether labeled with AnnexinV, TUNEL or Acridine Orange—we find them already inside microglia, suggesting that these cells are the only phagocytes active at this point in the fish brain. In the future it is going to be interesting to determine if and how glia and microglia share the task of finding and removing apoptotic neurons from the vertebrate brain.

Elegant cell culture studies of the phagocytic pathway have identified a large body of vital dyes that when applied to cells specifically label intracellular compartments. Remarkably, we were also able to use many of these tools simply by adding these dyes to the fish medium as microglial cells take up small chemical compounds and fluorescent dyes with great efficiency, allowing highly specific labeling of their intracellular processes. The use of dyes that emit fluorescence only when inside particular subcellular compartments, allowed a clear color-coding of the events from neuronal capture to digestion. The molecular regulators of these processes can be identified using both reverse and chemical genetic approaches. Taking advantage of these combined features, we have characterised the steps leading to neuronal phagocytosis within microglia via high-resolution imaging and identified the first molecule known to be required for their progression.

v-ATPase a1 Function in Microglia

The a1 subunit identified in this study is part of the large v-ATPase complex whose function is central in the acidification of all cellular compartments. However, by using live pH indicators, we show directly that in the absence of the a1 subunit activity internal vesicles have an acidic pH that is comparable to wild-type. How can the v-ATPase proton pump function in the absence of the a1 subunit? Interestingly, in many species the a1 subunit is encoded by several homologous genes and data from yeast and *C. elegans* suggest that these have specific functions, in distinct intracellular compartments and different cell types (Kawasaki-Nishi et al., 2003; Perzov et al., 2002; Pujol et al., 2001). Not surprisingly, in zebrafish there is at least one additional gene with high sequence similarity to the a1 subunit that could be responsible for the acidification of phagosomes in microglia (NP_001018502, showing 86% amino acid identity).

The a1 subunit has been previously identified as a mediator of vesicular fusion at the cell membrane during exocytosis. Our study demonstrates the first requirement of this molecule during endocytosis. We find that the a1 ATPase subunit is required for heterotypic fusion between phagosomes and lysosomes. In addition, two-color time-lapse imaging shows homotypic fusion events between phagosomes that form independently in different cell regions. Once again, these events require the activity of the a1 v-ATPase complex. The biological function of these phagosomal fusion events in microglia remains unclear. Similar phagosome-to-phagosome fusion have been observed in Dictyostelium, where phagosomes containing bacteria or latex beads fuse to form late multiple-particle compartments of unknown function (Duhon and Cardelli, 2002).

Studying Neuronal-Microglial Interactions during Brain Development

Microglia react promptly to neuronal degeneration and injury however very little is known about how these two cell types communicate at either the molecular or cellular level. To date, most studies have focused on the behavior of microglia after injury, however to improve our understanding of the role of these cells in diseased brains it is useful to better define their behavior under normal physiological conditions. To this aim, it is crucial to work with an intact in vivo system in which the normal morphology and dynamics of microglia are preserved. In the work described here, we have shown that microglia continuously phagocytose the large number of apoptotic neurons that are produced during normal brain development. Furthermore, in addition to understanding their behavior under normal physiological conditions, we can manipulate this developmental system, either genetically or pharmaceutically, in order to understand the immediate response of these cells to neuronal apoptosis. While there are perhaps differences in the precise behavior of microglia in pathological and developmental contexts, it is likely that there is significant overlap in the molecular and cellular machineries that allow them to recognize and engulf dying neurons.

One of the surprising findings of this work is that blocking the processing of engulfed material within the cell leads to changes in cellular morphology, which apparently feed back on behavior. By knocking-down the v0-ATPase a1 activity we block vesicular fusion, leading to the accumulation of phagosomes and indigested material. One interesting consequence of this defect is that the microglia appear to have "indigestion." It will be interesting to determine whether interfering with phagocytosis can reduce the devastating impact that microglia have in many neurodegenerative diseases.

EXPERIMENTAL PROCEDURES

Generation of ApoE-GFP Transgenic Line

GFP specific expression in microglia was achieved by inserting the lynEGFPpA marker (Köster and Fraser, 2001) in the *apolipoproteinE* locus via BAC (Bacterial Artificial Chromosome) homologous recombination in bacteria using the Red/ET Recombination Technology by Gene Bridges.

Generation of NBT-GFP Transgenic Line

The DsRed red-fluorescent-protein marker was cloned under the control of the NBT promoter (*Xenopus* neural-specific beta tubulin promoter). The resulting plasmid has been injected into one-cell embryos. The original construct NBT:MAPT-GFP was generated in Paul Krieg's lab and was a gift to Darren Gilmour from Enrique Amaya and Chi-Bin Chien.

Generation of pU1-Gal4-UAS-eGFP Transgenic Line

GFP-specific expression in the myeloid lineage was achieved by cloning 4kb of the pU1 promoter in front of the Gal4-UAS-eGFP cassette (Köster and Fraser, 2001).

atp6v0a1 Cloning

The zebrafish *atp6v0a1* (Accession number: NM_212672 and NP_997837) was amplified via PCR from wild-type cDNA by using the following primers:

atp6v0a1-1Forward: AGCTGTTTCGTAGCGAGGAG
atp6v0a1-1Reverse: GCAATTAATCGGCTCTCTCG
atp6v0a1-2Forward: TGGTGCTGAACCAGACAGAG
atp6v0a1-2Reverse:ACGCAGTGTTTGAGATGCAG

The resulting products were cloned into the pGEMT vector (Promega) and sequenced. Protein sequence has a predicted size of 116kDa and bares 82% identity with the human homolog (NP_005168) and 42% identity with the yeast homolog vph1 protein.

Morpholino Injections

Morpholino oligomers were obtained from Gene Tools Inc., diluted and injected in one-cell embryos. Morpholinos were injected at a concentration of 0.4 mM (ATG-MO and ATG-CO) and 0.3 mM (GT-MO and GT-CO).

atp6v0a1-MO: CCTCGCTACGAAACAGCTCCCCCAT
atp6v0a1-Co-MO: CCTgGCTAgGAAAgAGCTgCCCgAT
atp6v0a1-GT-MO GAAATGGTCTGCACTTACATCTCTG
atp6v0a1-GT-CO GAAATcGTgTGCAgTTAgATCTgTG

To test binding of the atp6v0a1-MO we have cloned its target sequence (AATTATTATGGGGGAGCTGTTTCGTAGCGAGGAG) upstream of the GFP and the 5-mismatched a1MO target sequence (AATTATTATGGGAGAGCTATTTCG-GAGTGAAGAG) upstream of the dTomato Both RNAs have been injected at a concentration of 50–100 ng/μl.

We have monitored the efficacy of splice-blocking MO using primers that flank the first intron which amplify a band of 180 bp in normally spliced cDNA. In cDNA prepared from pools of embryos injected with GT-MO a band shift of 1.5 kb could be observed,

The following primers were used:
Primer-F AGCTGTTTCGTAGCAGGAG
Primer-R CTGGAATGCGTTGACATCTG

In Situ Hybridization

In situ hybridization was carried out using an *apo-E* probe following the protocol described by Ober and Schulte-Merker (Ober and Schulte-Merker, 1999).

Combined Whole-Mount In Situ Hybridization and Antibody Staining

Fluorescent in situ hybridization was performed using *atp6v0a1* and *apoE* probes and following the Tyramide Signal Amplification method (PerkinElmer). Rabbit-anti GFP (1:500, Torrey Pines Biolabs) antibody was used for counterstaining of microglial in the ApoE-GFP background and myeloid cells in pU1-Gal4-UAS-GFP. We have followed the protocol described by Schneider and Granato (Schneider and Granato, 2006).

Microscopy and Imaging

For live imaging, embryos were anesthetized in 0.01% tricaine and embedded in 1.5% low-melting point agarose. Time-lapse analysis was carried out on a Zeiss 510 Meta and an Olympus FV1000 confocal microscope with 40×/NA1.2 objectives and the 488 nm, 543 nm and 650 nm laserlines respectively. Usually, 4 z-stacks spanning approximately 10 μm were captured and were then flattened by maximum projection in ImageJ.

Detection of Apoptosis

Apoptosis in living zebrafish embryos was detected using Acridine orange (Sigma), CaspGlow (BioCat) TMR-TUNEL (Roche) and AnnexinV-Cy5 (BioVision), a bright fluorescent reagent with strong affinity binding for phosphatidylserine (PS). This dye was added directly to the fish water at a concentration of 1/500, as suggested by the maker. In the pulse-chase experiment embryos were left in incubation with the AnnexinV-Cy5 dye for 2 hr and then extensively washed before mounting them under the microscope. Cy5 yields fluorescent with a imax of emission of 670 nm. Z-stacks of stage-matched microglia were captured using identical settings. A region of interest was defined using the Zeiss LSM Meta software. Fluorescence intensity profiles were generated using the MeanRoi option in the Zeiss LSM Software, and the values were plotted in Excel.

Staining of Acidic Organelles with LysoTracker Red DND-99

Organelles with low internal pH were labeled by adding directly to the fish water the LysoTracker DND-99 dye (Molecular Probes) at the suggested concentration of 70 nM. Embryos were incubated for 30 min with the LysoTracker prior mounting them under the microscope. As indicated by the maker LysoTracker DND-99 yields fluorescent in acidic compartments with a lmax emission of around 590 nm.

pH Acidity Measurement Using LysoSensor Green DND-189

Acidic pH was detected by adding directly to the fish water the LysoSensor DND-189 dye (Molecular Probes) at the suggested concentration of 1μM. Embryos were incubated for 5 min with the LysoSensor dye prior mounting them under the microscope. As indicated by the maker, the fluorescence intensity of the LysoSensor DND-189 at 505 nm reaches its maxima between pH 4 and 5. Z-stacks of stage-matched microglia were captured using identical settings. A region of interest was defined using the Zeiss LSM Meta software. Intensity profiles at 505 nm were generated using the MeanRoi option of the Zeiss LSM software and the values for several experiments were plotted in Excel.

Blocking v-Atpase Proton Pump Activity with the Bafylomicin A1 Inhibitor

Bafylomicin A1 (Sigma) inhibitor was added directly to the fish medium at a final concentration of 3 μM as indicated by the maker. The embryos were left in the incubation medium for 40 min before mounting them under the confocal microscope.

Staining of lysosomes with MR Cathepsin and DQ-BSA

MagicRed-Cathepsin (Immunochemistry Technologies, LLC) has been injected in the brain of 3-day-old embryos at the concentration suggested by the maker (1:260). DQ-BSA (Invitrogen) has been added directly to the fish medium (final concentration 1/10000). Adding to the fish medium 1%DMSO facilitated penetration of the dye.

Cloning of the CD63/Lysosomal-Associated-Membrane-Protein-3-GFP (CD-63-GFP)

The human *CD63* was a gift from Albert Haas and Gillian Griffiths. We have have cloned at the C-teminus of the EGFP into the pSC2 expression vector. RNA at a concentration of 60 ng was injected in 1 cell stage embryos.

Western Blot

Western blot analysis was performed in accord to the method described by Westerfield (Westerfield, 2000). Proteins extracts produced from around 100 3 dpf old embryos were separated in 10% polyacrylamide gels and transferred to Hybond ECL membranes (Amersham Pharmacia Biotech) by wet-blotting. For detection we have followed the standard method of ECL Western blotting detection (Amersham Pharmacia Biotech). The polyclonal V-ATPase a1

(H-140, Santa Cruz) was added at a concentration of 1/100 and for control we have used the anti-alpha-actin antibody from Dianova (1/1000).

SUPPLEMENTAL DATA

Supplemental Data include four figures and ten movies and can be found with this article online at http://www.cell.com/cgi/content/full/133/5/916/DC1/.

ACKNOWLEDGMENTS

We would like to thank Madeleine van Drenth and Darren Gilmour for the NBT-DsRed line. Albert Haas and Gillian Griffiths for the human CD63 clone. We are indebted to Maximiliano Gabriel Gutierrez for suggesting the lysosomal labeling techniques that proved so useful for this study. We would also like to thank Katrin Henke for helping with some of the stainings. We are grateful to Darren Gilmour, Michael Granato, and Gareth Griffiths for critical reading of the manuscript. F.P. was supported by a postdoctoral fellowship of the Ernst Schering Research Foundation (ESRF).

Received: June 21, 2007
Revised: February 29, 2008
Accepted: April 14, 2008
Published: May 29, 2008

REFERENCES

Barron, K. (1995). The microglial cell. A historical review. J. Neurol. Sci. *134*, 57–68.

Bayer, M.J., Reese, C., Buhler, S., Peters, C., and Mayer, A. (2003). Vacuole membrane fusion: V0 functions after trans-SNARE pairing and is coupled to the Ca2+-releasing channel. J. Cell Biol. *162*, 211–222.

Block, M.L., Zecca, L., and Hong, J.S. (2007). Microglia-mediated neurotoxicity: uncovering the molecular mechanisms. Nat. Rev. Neurosci. *8*, 57–69.

Blott, E.J., Bossi, G., Clark, R., Zvelebil, M., and Griffiths, G.M. (2001). Fas ligand is targeted to secretory lysosomes via a proline-rich domain in its cytoplasmic tail. J. Cell Sci. *114*, 2405–2416.

Bouvier, G., Benoliel, A.M., Foa, C., and Bongrand, P. (1994). Relationship between phagosome acidification, phagosome-lysosome fusion, and mechanism of particle ingestion. J. Leukoc. Biol. *55*, 729–734.

Bowman, E.J., Graham, L.A., Stevens, T.H., and Bowman, B.J. (2004). The bafilomycin/concanamycin binding site in subunit c of the V-ATPases from Neurospora crassa and Saccharomyces cerevisiae. J. Biol. Chem. *279*, 33131–33138.

Campbell, W.A., Yang, H., Zetterberg, H., Baulac, S., Sears, J.A., Liu, T., Wong, S.T., Zhong, T.P., and Xia, W. (2006). Zebrafish lacking Alzheimer presenilin enhancer 2 (Pen-2) demonstrate excessive p53-dependent apoptosis and neuronal loss. J. Neurochem. *96*, 1423–1440.

Desjardins, M., and Griffiths, G. (2003). Phagocytosis: latex leads the way. Curr. Opin. Cell Biol. *15*, 498–503.

de Saint-Vis, B., Vincent, J., Vandenabeele, S., Vanbervliet, B., Pin, S., Aït-Yahia, S., Patel, S., Mattei, M., Banchereau, J., and Zurawski, S. (2000). A Novel Lysosome-Associated Membrane Glycoprotein, DC-LAMP, Induced upon DC Maturation, Is Transiently Expressed in MHC Class II Compartment. Immunity *9*, 325–336.

Duhon, D., and Cardelli, J. (2002). The regulation of phagosome maturation in Dictyostelium. J. Muscle Res. Cell Motil. *23*, 803–808.

Geisow, M.J., d'Arcy Hart, P., and Young, M.R. (1981). Temporal changes of lysosome and phagosome pH during phagolysosome formation in macrophages: studies by fluorescence spectroscopy. J. Cell Biol. *10*, 645–652.

Grinstein, S., Nanda, A., Lukacs, G., and Rotstein, O. (1992). V-ATPases in phagocytic cells. j. Exp. Biol. *172*, 179–192.

Harris, E., and Cardelli, J. (2002). RabD, a Dictyostelium Rab14-related GTPase, regulates phagocytosis and homotypic phagosome and lysosome fusion. J. Cell Sci. *115*, 3703–3713.

Herbomel, P., Thisse, B., and Thisse, C. (1999). Ontogeny and behaviour of early macrophages in the zebrafish embryo. Development *126*, 3735–3745.

Herbomel, P., Thisse, B., and Thisse, C. (2001). Zebrafish early macrophages colonize cephalic mesenchyme and developing brain, retina, and epidermis through a M-CSF receptor-dependent invasive process. Dev. Biol. *238*, 274–288.

Hiesinger, P.R., Fayyazuddin, A., Mehta, S.Q., Rosenmund, T., Schulze, K.L., Zhai, R.G., Verstreken, P., Cao, Y., Zhou, Y., Kunz, J., and Bellen, H.J. (2005). The v-ATPase V0 subunit a1 is required for a late step in synaptic vesicle exocytosis in Drosophila. Cell *121*, 607–620.

Kawasaki-Nishi, S., Nishi, T., and Forgac, M. (2003). Proton translocation driven by ATP hydrolysis in V-ATPases. FEBS Lett. *545*, 76–85.

Kettenmann, H. (2007). Neuroscience: the brain's garbage men. Nature *446*, 987–989.

Koizumi, S., Shigemoto-Mogami, Y., Nasu-Tada, K., Shinozaki, Y., Ohsawa, K., Tsuda, M., Joshi, B.V., Jacobson, K.A., Kohsaka, S., and Inoue, K. (2007). UDP acting at P2Y6 receptors is a mediator of microglial phagocytosis. Nature *446*, 1091–1095.

Köster, R.W., and Fraser, S.E. (2001). Tracing transgene expression in living zebrafish embryos. Dev. Biol. *233*, 329–346.

Kuan, C.Y., Roth, K.A., Flavell, R.A., and Rakic, P. (2000). Mechanisms of programmed cell death in the developing brain. Trends Neurosci. *23*, 291–297.

Kurant, E., Axelrod, S., Leaman, D., and Gaul, U. (2008). six-microns under acts upstream of draper in the glial phagocytosis of apoptotic neurons. Cell *133*, 498–509.

Lauber, K., Blumenthal, S.G., Waibel, M., and Wesselborg, S. (2004). Clearance of apoptotic cells: getting rid of the corpses. Mol. Cell *14*, 277–287.

Liegeois, S., Benedetto, A., Garnier, J.M., Schwab, Y., and Labouesse, M. (2006). The V0-ATPase mediates apical secretion of exosomes containing Hedgehog-related proteins in Caenorhabditis elegans. J. Cell Biol. *173*, 949–961.

Liu, T.X., Howlett, N.G., Deng, M., Langenau, D.M., Hsu, K., Rhodes, J., Kanki, J.P., D'Andrea, A.D., and Look, T.A. (2003). Knockdown of Zebrafish Fancd2 Causes Developmental Abnormalities via p53-Dependent Apoptosis. Dev. Cell *5*, 903–914.

McNeil, P.L., Tanasugarn, L., Meigs, J.B., and Taylor, D.L. (1983). Acidification of phagosomes is initiated before lysosomal enzyme activity is detected. J. Cell Biol. *97*, 692–702.

Mellman, I., Fuchs, R., and Helenius, R. (1986). Acidification of the endocytic and exocytic pathways. Annu. Rev. Biochem. *55*, 663–700.

Muller, O., Bayer, M.J., Peters, C., Andersen, J.S., Mann, M., and Mayer, A. (2002). The Vtc proteins in vacuole fusion: coupling NSF activity to V(0) trans-complex formation. EMBO J. *21*, 259–269.

Nasevicius, A., and Ekker, S. (2000). Effective targeted gene 'knockdown' in zebrafish. Nat. Genet. *26*, 216–220.

Nijhawan, D., Honarpour, N., and Wang, X. (2000). Apoptosis in Neural Development and Disease. Annu. Rev. Neurosci. *23*, 73–87.

Nimmerjahn, A., Kirchhoff, F., and Helmchen, F. (2005). Resting Microglial Cells Are Highly Dynamic Surveillants of Brain Parenchyma in Vivo. Science *308*, 1314–1318.

Nishi, T., and Forgac, M. (2002). The vacuolar (H+) ATPases nature's most versatile proton pumps. Nat. Rev. Mol. Cell Biol. *3*, 94–103.

Ober, E., and Schulte-Merker, S. (1999). Signals from the yolk cell induce mesoderm, neuroectoderm, the trunk organizer, and the notochord in zebrafish. Dev. Biol. *215*, 167–181.

Parnaik, R., Raff, M., and Scholes, J. (2000). Differences between the clearance of apoptotic cells by professional and non-professional phagocytes. Curr. Biol. *10*, 857–860.

Perzov, N., Padler-Karavani, V., Nelson, H., and Nelson, N. (2002). Characterization of yeast V-ATPase mutants lacking Vph1p or Stv1p and the effect on endocytosis. J. Exp. Biol. *205*, 1209–1219.

Platt, N., da Silva, R.P., and Gordon, S. (1998). Recognizing death: the phagocytosis of apoptotic cells. Trends Cell Biol. *8*, 365–372.

Pujol, N., Bonnerot, C., Ewbank, J.J., Kohara, Y., and Thierry-Mieg, D. (2001). The Caenorhabditis elegans unc-32 gene encodes alternative forms of a vacuolar ATPase a subunit. J. Biol. Chem. *276*, 11913–11921.

Rhodes, J., Hagen, A., Hsu, K., Deng, M., Liu, T.X., Look, A.T., and Kanki, J.P. (2005). Interplay of pu.1 and gata1 determines myelo-erythroid progenitor cell fate in zebrafish. Dev. Cell *8*, 97–108.

Schneider, V.A., and Granato, M. (2006). The Myotomal diwanka (lh3) Glycosyltransferase and Type XVIII Collagen Are Critical for Motor Growth Cone Migration. Neuron *50*, 683–695.

Streit, W.J., and Kincaid-Colton, C.A. (1995). The brain's immune system. Sci. Am. *273*, 58–61.

Tsuda, M., Shigemoto-Mogami, Y., Koizumi, S., Mizokoshi, A., Kohsaka, S., Salter, M.W., and Inoue, K. (2003). P2X4 receptors induced in spinal microglia gate tactile allodynia after nerve injury. Nature *424*, 778–783.

Westerfield, M. (2000). The Zebrafish Book: A Guide of the Laboratory Use of the Zebrafish. (Eugene, OR: University of Oregon Press).